

# Phase diagram studies in the quasi binary systems $\text{LaMnO}_3\text{-SrMnO}_3$ and $\text{LaMnO}_3\text{-CaMnO}_3$

Peter Majewski, Lars Epple, Michael Rozumek, Heike Schluckwerder, and Fritz Aldinger  
*Max-Planck-Institut für Metallforschung, Pulvermetallurgisches Laboratorium, Heisenbergstraße 5,  
70569 Stuttgart, Germany*

(Received 20 August 1999; accepted 10 February 2000)

The quasi binary systems  $\text{LaMnO}_3\text{-SrMnO}_3$  and  $\text{LaMnO}_3\text{-CaMnO}_3$  were studied. Both systems show a miscibility gap at intermediate La:Sr and La:Ca ratios below about 1400 °C in air. This phenomenon causes the decomposition of single-phase  $(\text{La,Sr})\text{MnO}_{3-x}$  and  $(\text{La,Ca})\text{MnO}_{3-x}$  solid solution into La-rich  $\text{SrMnO}_{3-x}$  + Sr-rich  $\text{LaMnO}_{3-x}$  and La-rich  $\text{CaMnO}_{3-x}$  + Ca-rich  $\text{LaMnO}_{3-x}$  at lower temperatures, respectively. At 1400 °C in the system  $\text{LaMnO}_3\text{-SrMnO}_3$ , a structure transformation of  $(\text{La,Sr})\text{MnO}_3$  from orthorhombic to rhombohedral with increasing Sr content was not observed, and the structure of  $\text{La}_{0.7}\text{Sr}_{0.3}\text{MnO}_3$  was determined to be orthorhombic with  $a = 0.54927 \pm 0.0009$  nm,  $b = 0.54582 \pm 0.0009$  nm, and  $c = 0.76772 \pm 0.0034$  nm.

## I. INTRODUCTION

Sr- or Ca-doped  $\text{LaMnO}_{3-x}$  (LM) is of great technological interest for magnetic information storage systems due to its significant magnetoresistive properties.<sup>1</sup> In addition, high-temperature oxygen and electron conductivity as well as catalytic properties qualifies the compound to be a cathode material of solid oxide fuel cells (SOFC).<sup>2</sup> The maximum values of electron conductivity and magnetoresistivity have been observed for compositions with intermediate contents of alkaline earth elements.<sup>2,3</sup>

The binary systems  $\text{La}_2\text{O}_3\text{-Mn}_2\text{O}_3$ ,<sup>4</sup>  $\text{SrO-Mn}_2\text{O}_3$ ,<sup>5</sup> and  $\text{CaO-Mn}_2\text{O}_3$ <sup>6</sup> contain the perovskite-structured phase  $\text{ABO}_3$  with  $A = \text{Sr, Ca, or La}$  and  $B = \text{Mn}$ . The crystal structure of LM is a function of the  $\text{Mn}^{3+}/\text{Mn}^{4+}$  ratio. For LM with a high  $\text{Mn}^{4+}$  content, e.g., Sr- or Ca-doped LM, a rhombohedral structure has been reported for temperatures of 1000–1200 °C,<sup>3,4,7</sup> whereas, at a lower  $\text{Mn}^{4+}$  content (low Sr or Ca content), LM crystallizes in an orthorhombic structure.<sup>4,7</sup> Urushibara and co-workers<sup>3</sup> observed the phase transition of Sr-doped LM from the orthorhombic to the rhombohedral modification at 1200 °C in air at  $x_{\text{Sr}} = 0.175$ .

Mitchell and co-workers<sup>7</sup> observed that at lower  $\text{Mn}^{4+}$  content ( $x_{\text{Sr}}$  below 0.175) orthorhombic and rhombohedral LM coexist at 1000 °C in air.

For Ca-doped LM, a cubic<sup>8</sup> (at 950 °C) as well as orthorhombic structure was reported.<sup>9,10</sup>  $\text{SrMnO}_{3-x}$  (SM) exhibits a phase transformation from orthorhombic to orthorhombic distorted hexagonal at about 1400 °C and to hexagonal at 1035 °C due to uptake of oxygen with decreasing temperature combined with an increase of the  $\text{Mn}^{4+}$  content of the phase.<sup>11</sup> At 1200 °C in air the  $\text{Mn}^{4+}$  content is about 90%.<sup>11</sup>

The crystal structure of  $\text{CaMnO}_{3-x}$  (CM) is orthorhombic at high and low  $\text{Mn}^{4+}$  contents, but the cell parameters significantly vary with the  $\text{Mn}^{4+}$  content.<sup>12,13</sup>

LM and SM as well as LM and CM form complete solid-solution series at temperatures of about 1400 °C in air. The extent of solid solution at lower temperatures has not been studied. However, knowledge of the solid solubility at the operating temperature of solid oxide fuel cells and the synthesis temperature of Sr- or Ca-doped LM films (800–1000 °C) is of great interest for the reliability of LM electrodes during operation of fuel cells and for the preparation of single-phase thin films of LM materials.

In addition, recent studies of the magnetic phase diagram of Ca-doped LM suggest that ferromagnetic LM and antiferromagnetic CM co-exist at intermediate Ca contents.<sup>14</sup> Knowledge of the thermodynamic phase diagram LM–CM is eminent to clarify this phenomenon.

In this work the extents of the solid solutions  $(\text{La,Sr})\text{MnO}_{3-x}$  and  $(\text{La,Ca})\text{MnO}_{3-x}$  are studied using microprobe analysis and x-ray diffraction (XRD) measurements.

## II. EXPERIMENTAL

Samples with the compositions  $\text{La}_{0.5}\text{Sr}_{0.5}\text{MnO}_{3-x}$  and  $\text{La}_{0.5}\text{Ca}_{0.5}\text{MnO}_{3-x}$  were prepared by using  $\text{La}_2\text{O}_3$ ,  $\text{SrCO}_3$ ,  $\text{CaCO}_3$ , and  $\text{MnO}_2$  (purity > 99%), respectively. The powder mixtures were calcined at 1200 °C in air for 12 h, ground, and cold isostatically pressed. The samples were then sintered at 800, 900, 1000, 1200, 1300, 1350, and 1400 °C in air for 48 h with intermediate regrinding as well as pressing and finally furnace cooled to room temperature (batch 1). A second batch of samples with

the composition  $\text{La}_{0.5}\text{Sr}_{0.5}\text{MnO}_{3-x}$  and  $\text{La}_{0.5}\text{Ca}_{0.5}\text{MnO}_{3-x}$ , respectively, was sintered at 1400 °C in air and subsequently annealed at 1350, 1300, 1200, 1000, 900, and 800 °C in air for up to 500 h and furnace cooled (batch 2). In addition, samples with the composition  $\text{La}_{1-x}\text{Sr}_x\text{MnO}_{3-y}$  and  $\text{La}_{1-x}\text{Ca}_x\text{MnO}_{3-y}$  with  $0 \leq x \leq 1$  were prepared in air at 1200 as well as 1400 °C and at 1300 as well as 1400 °C, respectively.

In addition to the powder metallurgical synthesis, samples with the composition  $\text{La}_{0.5}\text{Sr}_{0.5}\text{MnO}_3$  were prepared by a modified glycine–nitrate process using urea as a fuel in order to clarify whether processing conditions influence the phase formation within the systems. For each sample, appropriate volumes were taken from defined aqueous stock solutions of the corresponding cation–nitrates and mixed. The amount of urea added was calculated by following a method by Jain, Adiga, and Verneker derived for complete combustion.<sup>15</sup> For the present synthesis, solutions rich in fuel (combustion parameter  $\Phi_e \approx 2$ ) were prepared. Excess water was evaporated from each solution until gelling, before the mixtures were transferred into covered alumina crucibles and placed into a box furnace. Thermal treatment was carried out in a one-step process by first bringing samples to the ignition temperature and subsequently to the annealing temperature chosen for a particular phase study. Annealing times were typically in the range of 25 to 50 h. All samples were furnace-cooled to room temperature.

The solidus line of the  $(\text{La,Ca})\text{MnO}_3$  solid solution was determined by differential thermal analysis (DTA) with a heating rate of 10 K/min between room temperature and 1500 °C and 3 K/min between 1500 and 1700 °C in air. Samples with different La:Ca ratios which were sintered at 1400 °C were measured.

Phase identifications were performed by using scanning electron microscopy (SEM) with EDX (Zeiss DSM 982 Gemini, Oberkochen, Germany) and XRD ( $\text{Cu K}\alpha_1$ , radiation, Siemens D-5000, Munich, Germany). The structure analyses were performed by using the Rietveld analysis program DBWS-9807.

### III. RESULTS

The samples prepared at temperatures above 1350 °C consist of single-phase  $(\text{La,Sr})\text{MnO}_{3-x}$  and  $(\text{La,Ca})\text{MnO}_{3-x}$  solid solutions, respectively. Below that temperature a miscibility gap between LM and SM as well as LM and CM has been observed not depending on the synthesis route.

Figure 1 shows a micrograph of the sample of batch 2 sintered at 1200 °C. Ca-containing LM with the composition  $\text{La}_{0.64}\text{Ca}_{0.36}\text{MnO}_3$  and La-containing CM with the composition  $\text{La}_{0.33}\text{Ca}_{0.67}\text{MnO}_3$  can be easily identified with the scanning electron microscope using EDX. This observation indicates that separated phases other than a

complete solid solution exist at that temperature. In Fig. 2 the section of the XRD pattern of the sample with the composition  $\text{La}_{0.5}\text{Ca}_{0.5}\text{MnO}_3$  shows the [220] reflections of CM and the [024] reflection of LM, which indicates the existence of LM and CM in the  $\text{La}_{0.5}\text{Ca}_{0.5}\text{MnO}_3$  sample at 1200 °C.

The decomposition of single-phase  $\text{La}_{0.5}\text{Sr}_{0.5}\text{MnO}_{3-x}$  (batch 1, prepared at 1400 °C in air) into LM and SM after annealing at 1200 °C also can be detected by the XRD pattern of the sample showing reflections of both phases, LM and SM (Fig. 3). The XRD pattern of SM indicate that at 1200 °C in air La-rich SM crystallizes in the orthorhombic distorted hexagonal modification

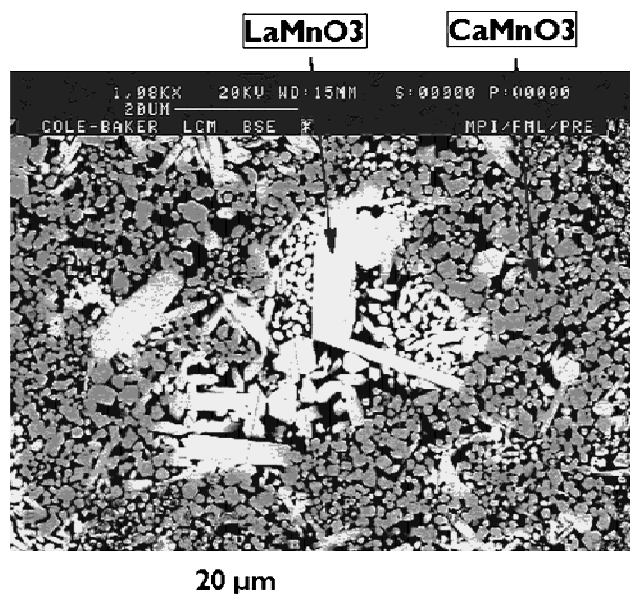


FIG. 1. Micrograph of a sample with the composition  $\text{La}_{0.5}\text{Ca}_{0.5}\text{MnO}_{3-x}$  at 1200 °C in air (batch 2).

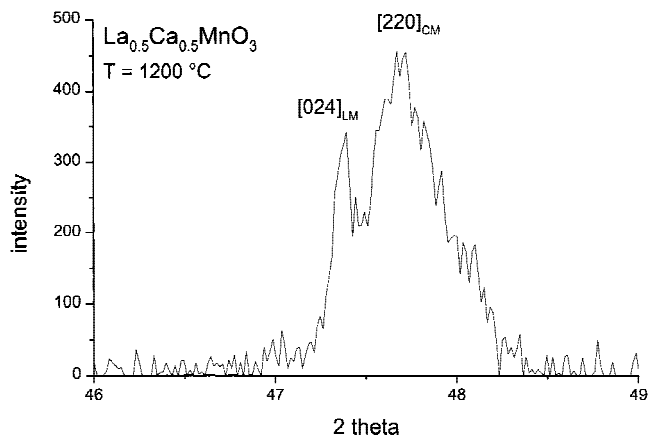


FIG. 2. Section of the XRD pattern of the sample  $\text{La}_{0.5}\text{Ca}_{0.5}\text{MnO}_{3-x}$  sintered at 1200 °C showing the [220] reflections of CM and the [024] reflection of LM (rhombohedral). (Orthorhombic structure of CM considered.)

determined by Ref. 8. EDX analysis of the sample confirms that the single-phase sample decomposes during the annealing at 1200 °C forming LM with the composition  $\text{La}_{0.62}\text{Sr}_{0.38}\text{MnO}_{3-x}$  and SM with the composition  $\text{La}_{0.36}\text{Sr}_{0.64}\text{MnO}_{3-x}$ . An additional annealing step of the same sample at again 1400 °C for 24 h results in the reaction of LM and SM into single-phase  $\text{La}_{0.5}\text{Sr}_{0.5}\text{MnO}_3$ .

In Figs. 4 and 5 the temperature concentration diagrams for the quasi binary system  $\text{LaMnO}_3\text{--SrMnO}_3$  and  $\text{LaMnO}_3\text{--CaMnO}_3$  show the miscibility gap between LM and SM as well as LM and CM at temperatures below 1400 °C in air determined mainly by SEM/EDX (see also Table I).

The DTA measurements indicate that the peritectic melting of the LM–CM solid solution depends on the La:Ca ratio. It increases with increasing La content (Fig. 5). The determined onset values of melting of the measured samples are listed in Table II.

At 1200 °C in air pure LM has found to be orthorhombic. The transformation of LM from orthorhombic to rhombohedral has been observed at a Sr content of about 0.2 at 1200 °C at (Fig. 6).

At 1400 °C the transition from the orthorhombic to the rhombohedral modification of Sr doped LM has not been observed. The Rietveld analysis of a sample with the composition  $\text{La}_{0.7}\text{Sr}_{0.3}\text{MnO}_{3-x}$  sintered at 1400 °C and quenched in air shows that Sr-doped LM is orthorhombic (Fig. 7, Table III). In the system LM–CM a phase transformation of Ca-doped LM was not observed. The obtained XRD patterns of the samples do not make it possible to distinguish between either orthorhombic or cubic structure.

At 1400 °C the increase of the Sr and Ca content of the solid solution, respectively, is reflected in a significant decrease of the *a*-axis parameter of LM (Fig. 8, Table IV).

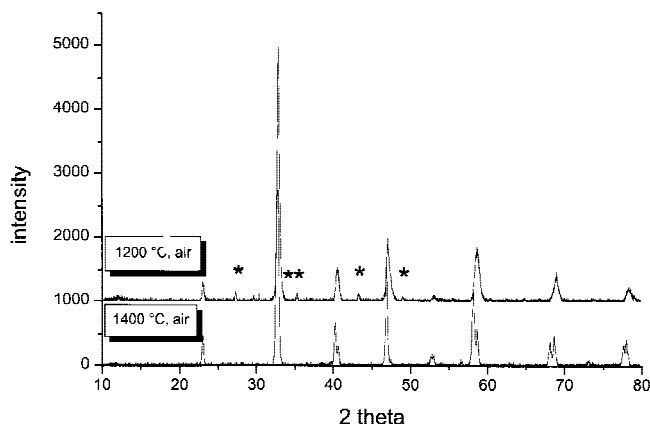


FIG. 3. XRD pattern of a sample with the composition  $\text{La}_{0.5}\text{Sr}_{0.5}\text{MnO}_{3-x}$  sintered at 1400 °C (bottom) and subsequently annealed at 1200 °C in air (batch 1). The stars mark reflections of  $\text{SrMnO}_3$ .<sup>8</sup> All other reflections can be attributed to  $\text{LaMnO}_3$ .

#### IV. DISCUSSION

The results of the experiments clearly show the occurrence of a miscibility gap between LM and SM as well as LM and CM at temperatures below about 1400 °C in air. The fact that the samples of batches 1 and 2 as well as the samples prepared with the glycine–nitrate process show the same results suggests that the observed phase contents of the samples represent thermodynamic equilibria. In addition, the fact that a multiphase sample with the composition  $\text{La}_{0.5}\text{Sr}_{0.5}\text{MnO}_3$  can be transformed into a single phase sample at 1400 °C and vice versa gives an additional evidence for thermodynamically stable conditions.

The occurrence of the miscibility gap between LM and SM appears to correlate with the phase transformations of Sr-doped LM from orthorhombic to rhombohedral with decreasing temperature. However, the reason for the miscibility gap between LM and CM is still not clarified but may be caused by a transformation from orthorhombic to cubic structure of Ca doped LM with decreasing temperature.

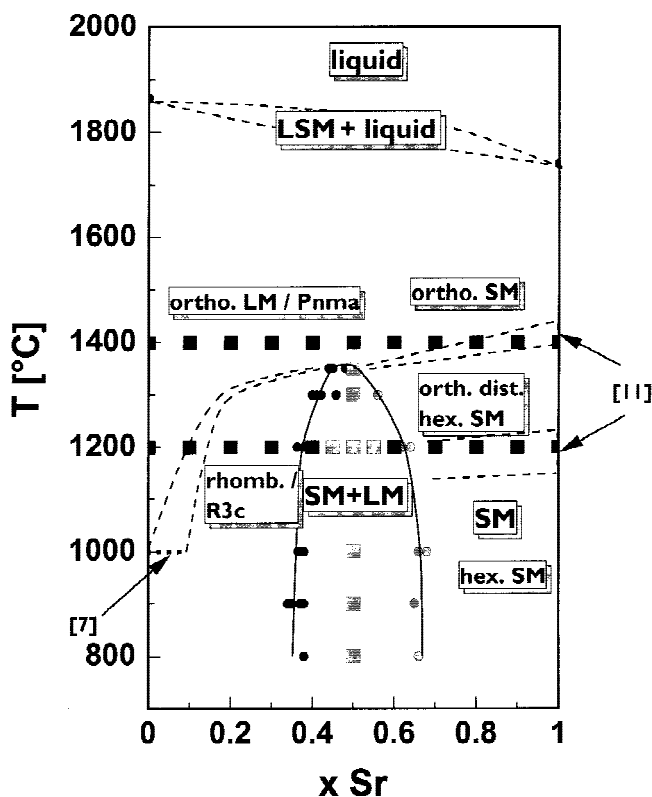


FIG. 4. Temperature–concentration diagram of the quasi binary system  $\text{SrMnO}_3\text{--LaMnO}_3$ : black squares, single-phase samples; gray squares, multiphase samples, results of EDX analysis of LM (black dots) and SM (gray dots) of the samples of batch 1 and 2. The melting temperature of LM is after Ref. 4, and that of SM, after Ref. 5.

The decomposition reaction below 1400 °C is slow, and therefore, it does not affect the material during furnace cooling. Annealing times of above 100 h are necessary to decompose the single-phase samples into two phase samples at 1200 °C in air.

The decrease of the *a*-axis parameter of the (La,Sr)MnO<sub>3-x</sub> solid solution with increasing Sr content cannot be explained with the known volume requirement of the ions considering ionic radii for eightfold coordination: La<sup>3+</sup>, 116 pm; Sr<sup>2+</sup>, 266 pm.<sup>16</sup> This decrease may be caused by the decrease of the ion size of Mn with increasing oxidation state. The differences in the determined axis parameters of the different groups is probably due to different Mn<sup>3+</sup>/Mn<sup>4+</sup> ratios of LM of the prepared samples.<sup>4,7</sup> The significant decrease of the *a*-axis parameter with increasing Ca content of LM is supposedly due to both the decrease of the ion size of Mn and the smaller volume requirement of the Ca<sup>2+</sup> ion (100 pm) compared to the La<sup>3+</sup> ion.<sup>16</sup>

The observed transformation of doped LM from orthorhombic to rhombohedral at 1200 °C is in agreement with the results of Refs. 3 and 7. At temperatures

above 1350 °C a transformation of LM from orthorhombic to rhombohedral with increasing Sr content has not been observed. Therefore, it is assumed that orthorhombic LM is the high-temperature modification of Sr-substituted LM.

As the orthorhombic to rhombohedral phase transformation of Sr-doped LM is due to an increase of the Mn<sup>3+</sup>:Mn<sup>4+</sup> ratio, the question arises why rhombohedral LM is not stable above 1350 °C. The reason is believed to be a decreased oxygen content of LM at high temperature which stabilizes the orthorhombic modification of LM. This effect is also known from SM.<sup>11</sup> So, a detailed analysis of the oxygen content of Sr-doped LM as a function of the temperature is necessary to clarify this.

### V. CONCLUSIONS

With respect to the high operating temperatures (800–1000 °C) and long operating times (about 50,000 h) of SOFC, decomposition of LM could be important for the

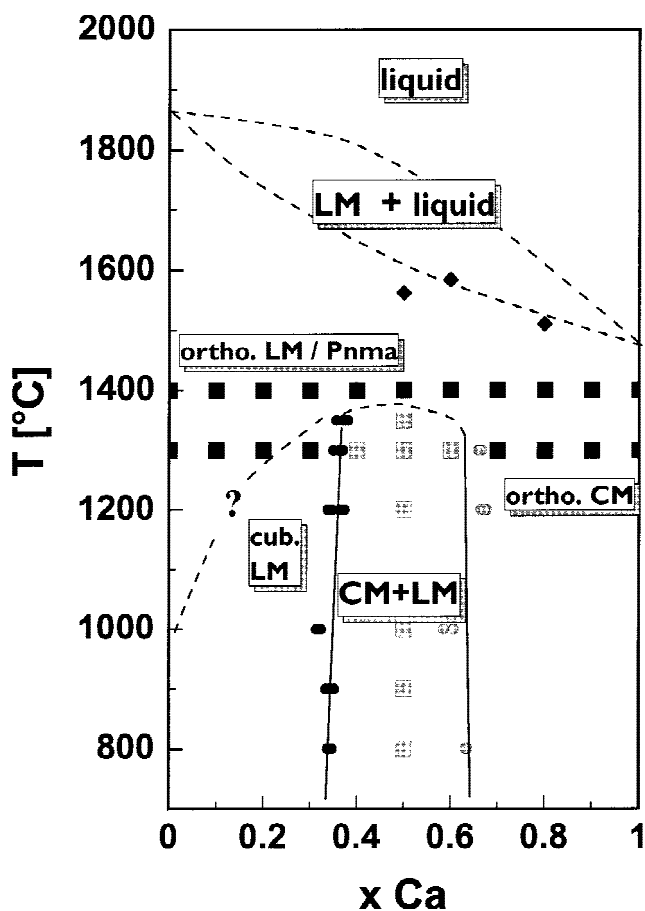


FIG. 5. Temperature–concentration diagram of the quasi binary system CaMnO<sub>3</sub>-LaMnO<sub>3</sub>. Black diamonds: temperature of the onset of melting determined by DTA measurements. For all other symbols, see Fig. 4 caption. The melting temperature of CM is after Ref. 6.

TABLE I. Analyzed La:Sr and La:Ca ratios of LM, SM, and CM versus temperature. Data points refer to Figs. 4 and 5.

T (°C)	SM (La:Sr)	LM (La:Sr)	CM (La:Ca)	LM (La:Ca)
1400		51:49		49:51
		50:50		50:50
		51:49		
1350		52:48		62:38
		55:45		62.5:37.5
		56:44		63:37
				64.5:35.5
1300	44:56	54:46	33.5:66.5	63:37
		58:42	34:66	64:36
		59:41	34:66	65:35
		60:40		
1200	36:64	62:38	32:68	63:37
	38:62	64:36	33:67	64:36
1000			34:66	65:35
	32:68	62:38	39:61	67.5:32.5
	34:66	63:37	41:59	68:32
		66:34		68.5:31.5
900	35:65	62:38		66:35
		63:37		66:34
		65:35		68.5:33.5
800	34:66	62:38	36.5:63.5	65:35
			37:63	65.5 34.5
				66:34

TABLE II. Determined temperature of the onset of peritectic melting of Ca-doped LM.

T (°C)	La:Ca ratio		
	0.2:0.8	0.4:0.6	0.5:0.5
	1504	1584	1562

reliability of the cathode material. The experiment shows that a decomposition of Sr- or Ca-substituted LM is detectable after only 100 h at 900–1200 °C indicating that the decomposition of LM occurs at the beginning of the operating time of a SOFC which is expected to be 5–10 years. Even the properties of the cathode could be significantly affected by the decomposition, as La-doped SM has poor electron-conducting properties. Therefore, for the design of LM cathodes of solid oxide fuel cells and Sr- and Ca-doped LM films Sr contents of below La<sub>0.65</sub>(Sr/Ca)<sub>0.35</sub>MnO<sub>3-x</sub> have to be considered to avoid decomposition.

The existence of a miscibility gap influences the interpretation of magnetic phase diagrams of Sr- or Ca-doped LM. In samples with intermediate compositions prepared at temperatures below about 1400 °C ferromagnetic LM exists beside antiferromagnetic SM and CM, respectively. This aspect has to be taken into account for the drawing of magnetic phase diagrams of LM. The

TABLE III. Crystallographic data for orthorhombic Sr-doped LM prepared at 1400 °C (see Fig. 11).

No.	hkl	d value		2θ	
		observed	calculated	observed	calculated
1	110	3.87000	3.87167	22.961	22.951
2	200	2.74600	2.74635	32.581	32.577
3	020	2.72900	2.72910	32.790	32.788
4	202	2.23400	2.23357	40.339	40.347
5	022	2.22400	2.22425	40.528	40.523
6	220	1.93700	1.93584	46.864	46.894
7	310	1.73600	1.73585	52.662	52.686
8	130	1.72750	1.72712	52.961	52.973
9	312	1.58150	1.58165	58.294	58.288
10	204	1.57300	1.57320	58.640	58.631
11	400	1.37350	1.37318	68.224	68.242
12	040	1.36540	1.36455	68.685	68.734
13	224	1.36300	1.36296	68.823	68.825
14	402	1.29320	1.29294	73.116	73.133
15	420	1.22700	1.22665	77.772	77.798
16	332	1.22370	1.22327	78.021	78.054
17	240	1.22260	1.22202	78.105	78.149

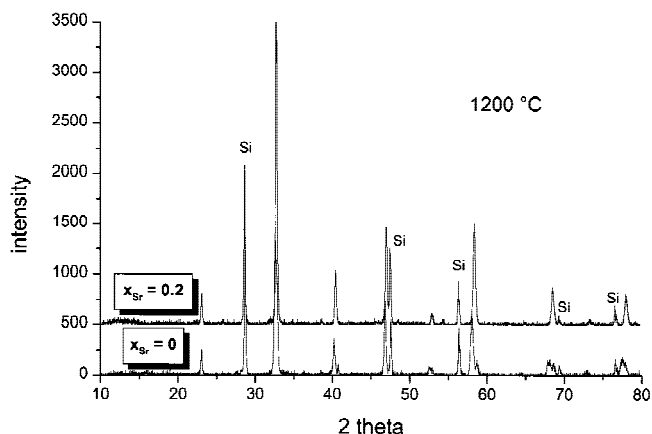


FIG. 6. XRD pattern of LaMnO<sub>3</sub> and La<sub>0.8</sub>Sr<sub>0.2</sub>MnO<sub>3-x</sub> sintered at 1200 °C in air.

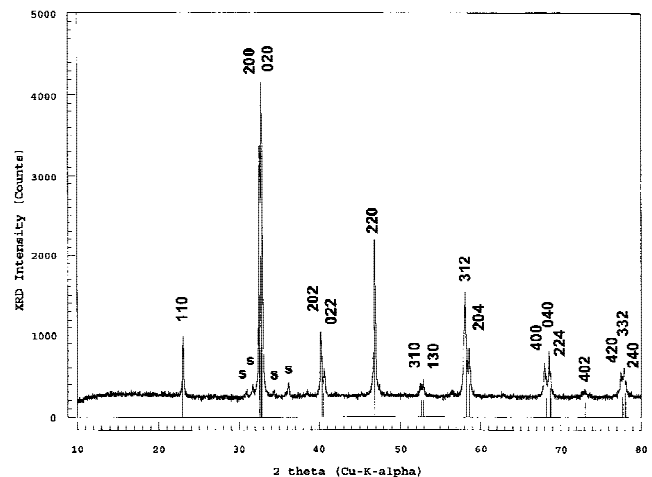


FIG. 7. Rietveld analysis of orthorhombic samples with the composition La<sub>0.7</sub>Sr<sub>0.3</sub>MnO<sub>3-x</sub> sintered at 1400 °C in air. S: sample holder.

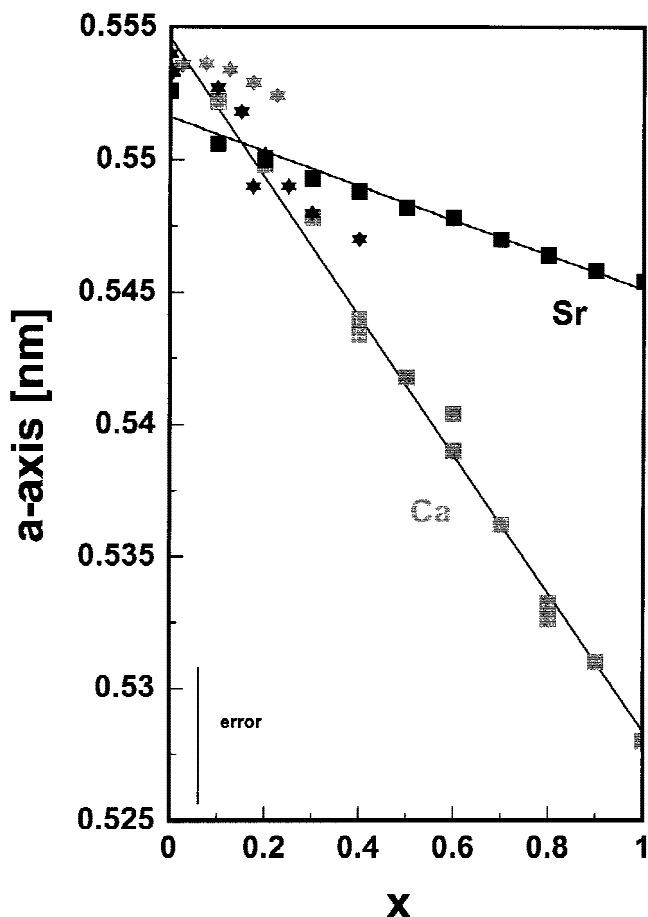


FIG. 8. *a*-axis parameter versus the Sr content of LM solid solution: black squares, Sr-doped LM, this work; gray squares, Ca-doped LM, this work; black stars, Ref. 3; gray squares, Ref. 7.

TABLE IV. Determined *a*-axis parameter of orthorhombic Sr- and Ca-doped LM prepared at 1400 °C.

La:Sr ratio	<i>a</i> axis (nm)	La:Ca ratio	<i>a</i> axis (nm)
1:0	0.5526		
0.9:0.1	0.5506	0.9:0.1	0.5522
0.8:0.2	0.5500	0.8:0.2	0.5500
0.7:0.3	0.5493	0.7:0.3	0.5478
0.6:0.4	0.5488	0.6:0.4	0.5437
0.5:0.5	0.5482	0.5:0.5	0.5418
0.4:0.6	0.5478	0.4:0.6	0.5402
0.3:0.7	0.5470	0.3:0.7	0.5362
0.2:0.8	0.5464	0.2:0.8	0.5329
0.1:0.9	0.5458	0.1:0.9	0.5316
0:1	0.5454	0:1	0.5280

observed rhombohedral to orthorhombic phase transition of LM with intermediate Sr content with increasing temperature allows one to study the influence of the crystal structure of LM on its magnetoresistive properties at constant Sr content. However, with respect to the system SrMnO<sub>3</sub>-SrMnO<sub>2.5</sub>,<sup>6</sup> a possible temperature dependence of the oxygen content of LM has to be taken into account which could influence the Mn<sup>3+</sup>:Mn<sup>4+</sup> ratio of LM and its magnetoresistive properties.

#### ACKNOWLEDGMENT

The authors thank A. Cuneit Tas, Middle East University of Ankara, on leave at Max-Planck-Institut für Metallforschung, Stuttgart, Germany, for assistance at Rietveld analysis.

#### REFERENCES

1. C.N.R. Rao, A.K. Cheetham, and R. Mahesh, *Chem. Mater.* **8**, 2421 (1996).
2. *Proceedings of the Third International Symposium on Solid Oxide Fuel Cells*, edited by S.C. Singhal and H. Iwahara (The Electrochemical Society, Pennington, NJ, 1993).
3. A. Urushibara, Y. Moritomo, T. Arima, A. Asamitsu, G. Kido, and Y. Tokura, *Phys. Rev. B* **51**, 14103 (1995).
4. J.A.M. van Roosmalen, P. van Vlaanderen, E.H.P. Cordfunke, W.L. Ijdo, and D.J.W. Ijdo, *J. Solid State Chem.* **114**, 516 (1995).
5. T. Negas, *J. Solid State Chem.* **7**, 85 (1973).
6. H.S. Horowitz and J.M. Longo, *Mater. Res. Bull.* **13**, 1359 (1978).
7. J.F. Mitchell, D.N. Argyriou, C.D. Potter, D.G. Hinks, J.D. Jorgensen, and S.D. Bader, *Phys. Rev. B* **54**, 6172 (1996).
8. R. Mahendrian, R. Mahesh, N. Rangavittal, S.K. Tewari, A.K. Raychaudhuri, T.V. Ramakrishnan, and C.N.R. Rao, *Phys. Rev. B* **53**, 3348 (1995).
9. J. Kaduk and W. Wong-Ng, Powder Diffraction File, Card No. 49-0416, International Center for Diffraction Data (1993).
10. D. Grier and G. McCarthy, Powder Diffraction File, Card No. 46-0513, International Center for Diffraction Data (1993).
11. T. Negas and R.S. Roth, *J. Solid State Chem.* **1**, 409 (1970).
12. J.B. MacChesney, H.J. Williams, J.F. Potter, and R.C. Sherwood, *Phys. Rev.* **164**, 779 (1967).
13. K.R. Poeppelmeier, M.E. Leonowicz, and J.M. Longo, *J. Solid State Chem.* **44**, 89 (1982).
14. P. Schiffer, A.P. Ramirez, W. Bao, and S.W. Cheong, *Phys. Rev. Lett.* **53**, 3336 (1996).
15. S.R. Jain, K.C. Adiga, and V.R. Pai Verneker, *Combust. Flame* **40**, 71 (1981).
16. *Periodic Table on the Elements* (VCH, Weinheim, Germany, 1993).